

# A Genome-wide *Drosophila* Screen for Heat Nociception Identifies $\alpha 2\delta 3$ as an Evolutionarily Conserved Pain Gene

G. Gregory Neely,<sup>1,2,18</sup> Andreas Hess,<sup>3,18</sup> Michael Costigan,<sup>4</sup> Alex C. Keene,<sup>5</sup> Spyros Goulas,<sup>1</sup> Michiel Langeslag,<sup>6</sup> Robert S. Griffin,<sup>7</sup> Inna Belfer,<sup>8</sup> Feng Dai,<sup>8</sup> Shad B. Smith,<sup>9</sup> Luda Diatchenko,<sup>9</sup> Vaijayanti Gupta,<sup>10</sup> Cui-ping Xia,<sup>1</sup> Sabina Amann,<sup>1</sup> Silke Kreitz,<sup>3</sup> Cornelia Heindl-Erdmann,<sup>3</sup> Susanne Wolz,<sup>3</sup> Cindy V. Ly,<sup>11</sup> Suchir Arora,<sup>10</sup> Rinku Sarangi,<sup>10</sup> Debasis Dan,<sup>10</sup> Maria Novatchkova,<sup>1</sup> Mark Rosenzweig,<sup>12</sup> Dustin G. Gibson,<sup>9</sup> Darwin Truong,<sup>1</sup> Daniel Schramek,<sup>1</sup> Tamara Zoranovic,<sup>1</sup> Shane J.F. Cronin,<sup>1</sup> Belinda Angjeli,<sup>1</sup> Kay Brune,<sup>3</sup> Georg Dietzl,<sup>13</sup> William Maixner,<sup>9</sup> Arabella Meixner,<sup>1</sup> Winston Thomas,<sup>14</sup> J. Andrew Pospisilik,<sup>15</sup> Mattias Alenius,<sup>16</sup> Michaela Kress,<sup>6</sup> Sai Subramaniam,<sup>10</sup> Paul A. Garrity,<sup>12</sup> Hugo J. Bellen,<sup>17</sup> Clifford J. Woolf,<sup>4,\*</sup> and Josef M. Penninger<sup>1,\*</sup>

<sup>1</sup>Institute of Molecular Biotechnology of the Austrian Academy of Sciences, Dr. Bohr Gasse 3-5, A-1030 Vienna, Austria

<sup>2</sup>Neuroscience Program, Garvan Institute of Medical Research, 384 Victoria Street, Darlinghurst, Sydney, New South Wales 2010, Australia

<sup>3</sup>Department of Experimental and Clinical Pharmacology and Toxicology, University of Erlangen-Nuremberg, Fahrstrasse 17, 91054 Erlangen, Germany

<sup>4</sup>Program in Neurobiology, Children's Hospital Boston and Department of Neurobiology, Harvard Medical School, Boston, MA 02115, USA

<sup>5</sup>Biology Department, New York University, 100 Washington Square East, New York, NY 10003, USA

<sup>6</sup>Division of Physiology, Department of Physiology and Medical Physics, Innsbruck Medical University, Fritz-Pregl-Strasse 3, A-6020 Innsbruck, Austria

<sup>7</sup>Department of Anesthesia and Critical Care, Massachusetts General Hospital and Harvard Medical School, Boston, MA 02129, USA

<sup>8</sup>Molecular Epidemiology of Pain Program, Department of Anesthesiology, University of Pittsburgh, Pittsburgh, PA, USA

<sup>9</sup>Center for Neurosensory Disorders, University of North Carolina at Chapel Hill, Chapel Hill, NC 27599, USA

<sup>10</sup>Strand Life Sciences Pvt. Ltd., 237 C V Raman Avenue, Rajmahal Vilas, Bangalore, India

<sup>11</sup>Department of Neuroscience, Baylor College of Medicine, Houston, TX 77030, USA

<sup>12</sup>National Center for Behavioral Genomics, Department of Biology, Brandeis University, Waltham, MA 02458, USA

<sup>13</sup>Howard Hughes Medical Institute, Stanford University, 318 Campus Drive, Stanford, CA 94305, USA

<sup>14</sup>Deltagen, Inc., 1900 South Norfolk Street, Suite 105, San Mateo, CA 94403, USA

<sup>15</sup>Max Planck Institute for Immunobiology, Stuebeweg 51, D-79108 Freiburg, Germany

<sup>16</sup>Department of Clinical and Experimental Medicine, Linkoping University, Linkoping, SE-581 85, Sweden

<sup>17</sup>HHMI, Department of Molecular and Human Genetics, Department of Neuroscience and Program in Developmental Biology, Baylor College of Medicine, Houston, TX 77030, USA

<sup>18</sup>These authors contributed equally to this work

\*Correspondence: clifford.woolf@childrens.harvard.edu (C.J.W.), josef.penninger@imba.oeaw.ac.at (J.M.P.)

DOI 10.1016/j.cell.2010.09.047

## SUMMARY

Worldwide, acute, and chronic pain affects 20% of the adult population and represents an enormous financial and emotional burden. Using genome-wide neuronal-specific RNAi knockdown in *Drosophila*, we report a global screen for an innate behavior and identify hundreds of genes implicated in heat nociception, including the  $\alpha 2\delta$  family calcium channel subunit *straightjacket* (*stj*). Mice mutant for the *stj* ortholog *CACNA2D3* ( $\alpha 2\delta 3$ ) also exhibit impaired behavioral heat pain sensitivity. In addition, in humans,  $\alpha 2\delta 3$  SNP variants associate with reduced sensitivity to acute noxious heat and chronic back pain. Functional imaging in  $\alpha 2\delta 3$  mutant mice revealed impaired transmission of thermal pain-evoked signals from the thalamus to higher-order pain centers. Intriguingly, in  $\alpha 2\delta 3$  mutant mice, thermal

pain and tactile stimulation triggered strong cross-activation, or synesthesia, of brain regions involved in vision, olfaction, and hearing.

## INTRODUCTION

Acute and chronic pain affects millions of people after injury or surgery and those suffering from diseases like arthritis, cancer, and diabetes. Nociception (the detection of noxious or damaging stimuli) serves a crucial biological purpose: it alerts living organisms to environmental dangers, inducing the sensation of pain, reflex withdrawal, and complex behavioral and emotional responses, which protect the organism from further damage (Cox et al., 2006). Noxious stimuli are detected by specialized high-threshold primary sensory neurons (nociceptors) (Lumpkin and Caterina, 2007), which transfer signals to the spinal cord and then transmit them to the brain for higher-level processing that results in the conscious awareness of the sensation called pain (Tracey and Mantyh, 2007). The

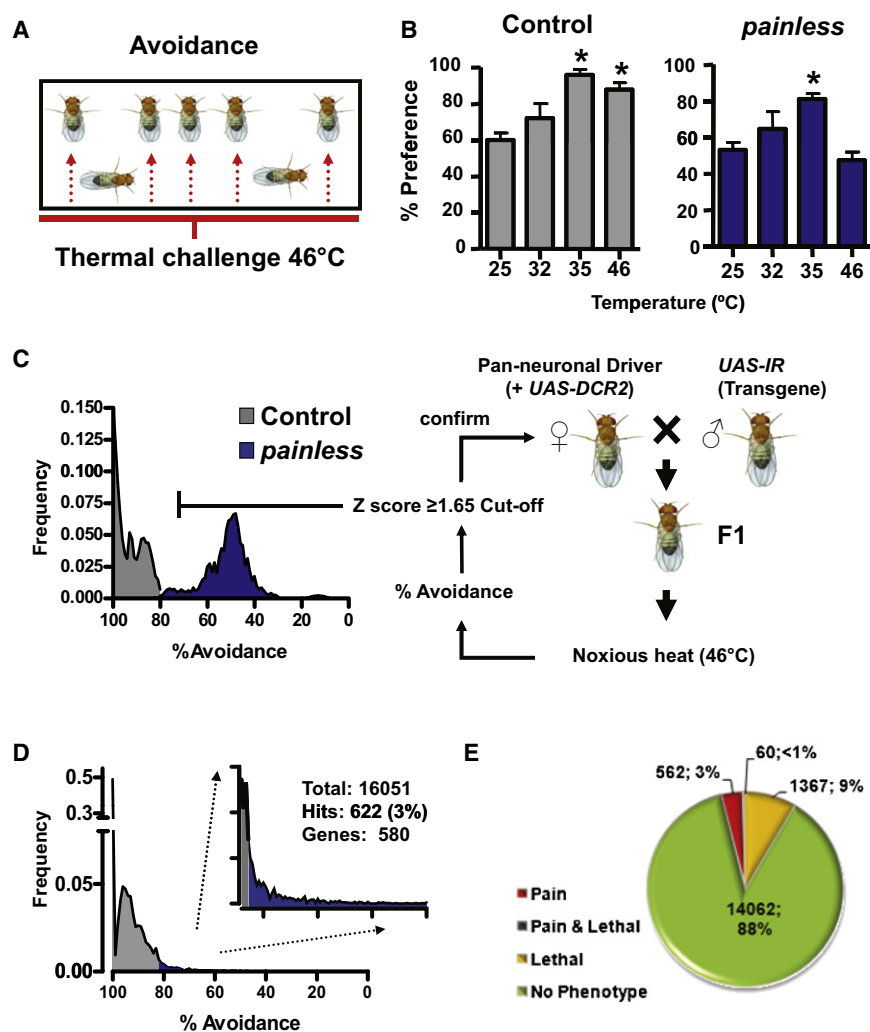


**Figure 1. Thermal Nociception in Adult *Drosophila***

(A) Schematic representation of the thermal nociception assay in adult *Drosophila*.

(B) Avoidance of noxious temperature of 46°C, but not avoidance of “subnoxious” temperatures (25°C–35°C), is impaired in *painless* mutant (*Painless*(EP(2)2451) flies compared to the control strain Canton S (control). Data are presented as mean values  $\pm$  SEM. Approximately 20 flies were tested per group in replicates of at least four cohorts. Significant differences ( $p < 0.001$ ) were observed for temperature and strain responses. Further post hoc (Tukey’s) analysis showed a significant temperature avoidance response at 46°C for control ( $p < 0.05$ ), but not *painless* flies when compared to responses at 25°C.

(C) To set up the experimental screening system, *w<sup>1118</sup>* (isogenic to the UAS-IR library)  $\times$  *elav-Gal4* flies (control, gray;  $n = 1706$ ) and *painless* mutant flies (*painless*, blue;  $n = 1816$ ) were tested for avoidance to noxious heat (46°C). Based on these data, a Z score  $\geq 1.65$  was calculated as a specific cutoff to identify lines for further screening. *Elav-Gal4* (also containing UAS-*Dicer 2* [UAS-*DRC2*] for more efficient gene silencing) females were crossed to UAS-IR lines to knock down the target genes in all neurons. All lines that exhibited a thermal avoidance defect (Z score  $\geq 1.65$ ) were retested multiple times.

(D) Results of the genome-wide screen. Approximately three percent (622 transformants) of total lines tested (16,051) exhibited a defect in thermal nociception, resulting in 580 candidate pain genes (622 transgenic lines).

(E) Distribution of adult thermal nociception and developmental lethal hits for 16,051 *Drosophila* UAS-IR lines. 1427 *elav-Gal4*  $\times$  UAS-IR lines were developmentally lethal (lethal). Among the 14624 viable lines, 562 lines exhibited defective thermal nociception (pain). An additional 60 lines that exhibited defective nociception as well as a semilethal phenotype were labeled as pain and lethal.

See also Figure S1 and Table S1.

functional importance of pain perception is exemplified by individuals with defects in nociception; patients with congenital insensitivity to pain do not survive past their twenties (Basbaum et al., 2009).

*Drosophila* (fruit flies) respond to noxious stimuli and have become a powerful model organism for studying the genetics of nociception (Manev and Dimitrijevic, 2004; Tracey et al., 2003; Xu et al., 2006). For instance, the TRP channel *PAINLESS* was identified as a heat-responsive channel mediating thermal-based nociception in fly larvae (Sokabe et al., 2008; Tracey et al., 2003). Using genome-wide neuronal-specific RNAi knockdown, we report a global screen for an innate behavior and identify hundreds of novel genes implicated in heat nociception in the fly, including the  $\alpha 2\delta$  family calcium channel subunit *straight-jacket*. Conservation of the mammalian straightjacket ortholog,  $\alpha 2\delta 3$ , in thermal nociception was confirmed in knockout mice that exhibit significantly impaired basal heat pain sensitivity and delayed thermal hyperalgesia after inflammation. In humans,

we found single-nucleotide polymorphisms (SNPs) in  $\alpha 2\delta 3$  that are associated with reduced acute heat pain sensitivity in healthy volunteers and chronic postsurgical back pain.

## RESULTS

### A Genome-wide Screen for Thermal Nociception

To identify genes required for nociception, we developed a high-throughput behavioral assay to determine the response of adult *Drosophila* to noxious heat as a stimulus. When exposed to a surface at a constant temperature of 25°C, flies distribute evenly in the experimental chamber, but when given a choice between a noxious (46°C) and nonnoxious (31°C) surface, flies rapidly avoid the harmful temperature (Figures 1A and 1B). *painless* mutant flies respond normally to subnoxious temperatures ( $\leq 39^\circ\text{C}$ ) but fail to avoid noxious heat (46°C) (Figure 1B). Thus, adult flies can rapidly avoid noxious heat, and this complex innate behavior is dependent on *painless*.

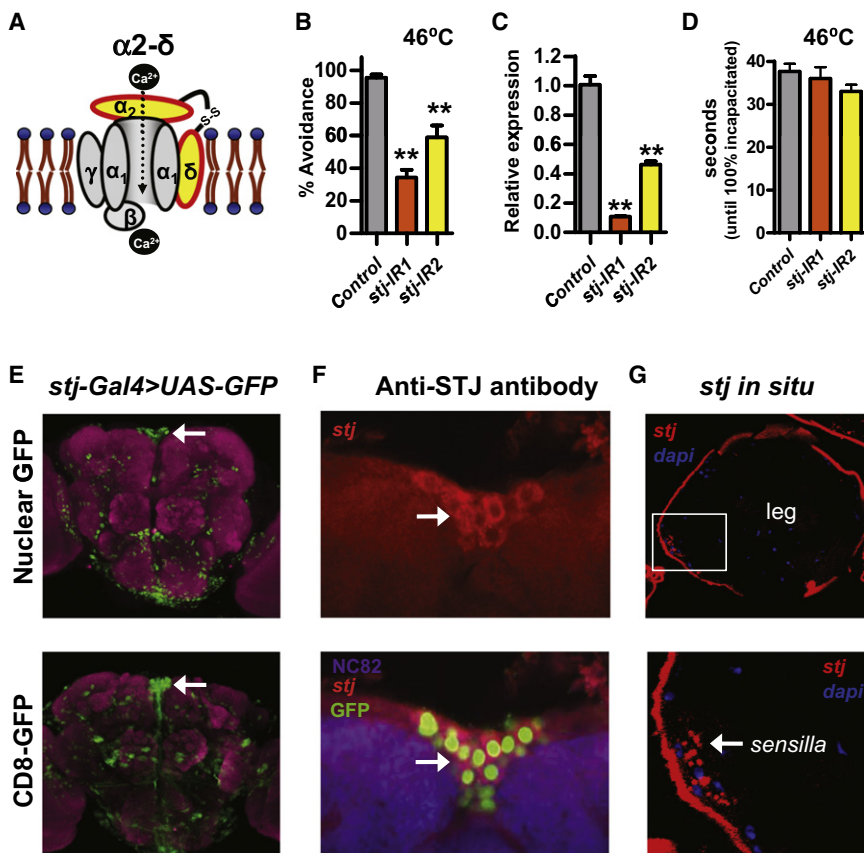


**Figure 2. Straightjacket Controls Thermal Nociception in Adult *Drosophila***

(A) Diagram of the  $\alpha 2\text{-}\delta$  family encoding peripheral subunits of  $\text{Ca}^{2+}$  channels.

(B) RNAi knockdown of *stj* impairs noxious thermal avoidance in adult *Drosophila* (percent avoidance of noxious temperature). *stj-IR1* = inverted repeat 1, *stj-IR2* = inverted repeat 2, both crossed to *elav-Gal4;UAS-DCR2*.

(C) Q-PCR for *stj* knockdown efficiency in *elav-Gal4 > UAS-stj-IR1/2* adult fly brains.

(D) Kinetics of temperature-induced paralysis for control and *elav-Gal4 > UAS-stj* flies.

(E) *stj-Gal4* driving expression of lamin:GFP to label nuclei and cell surface CD8:GFP to visualize axonal projections in the brain of adult flies. The pars intercerebralis is marked with an arrow.

(F) Colocalization of anti-STJ immunostaining and *stj-Gal4 > UAS-lamin:GFP*. The pars intercerebralis is marked with an arrow.

(G) *stj in situ* hybridization in the leg of wild-type ( $w^{1118}$ ) flies. Of note, the sense control did not show any signal. DAPI counterstaining is shown as mark nuclei. All data are presented as mean  $\pm$  SEM. \* $p < 0.05$ ; \*\* $p < 0.01$  (Student's *t* test). See also Figure S2.

Using this assay, we performed a genome-wide behavioral screen using the Vienna global *Drosophila* RNAi library (Dietzl et al., 2007). The panneuronal-specific *elav-Gal4* driver line was crossed to flies containing *UAS-IR* (IR, inverted repeat) transgenes covering the expressed genome (Figure 1C). Testing control flies ( $n = 1706$ ) over many different days revealed that the vast majority avoided the noxious surface, with a mean avoidance response of  $92\% \pm 6.4\%$  SD, whereas *painless* mutants ( $n = 1816$ ) exhibited a markedly reduced avoidance response ( $51\% \pm 9.97\%$  SD). Based on these data, we set our primary cutoff at the 95 percentile of probability, corresponding to a Z score of  $> 1.65$  (Figure 1C). At this threshold, we consistently observed impaired thermal nociception in *painless* mutant flies.

To identify novel genes regulating pain, we tested 16051 *elav-Gal4 > UAS-IR* combinations targeting 11664 different *Drosophila* genes (82% of the *Drosophila* genome version 5.7) for effects on noxious temperature avoidance (Figure 1D and Figure S1B available online). Positive hits were retested, and 622 specific transgenic *UAS-IR* lines corresponding to 580 genes were identified as candidate thermal nociception genes (Figure 1E and Tables S1A–S1C). Approximately 9% of the neuronal *elav-Gal4*-driven *UAS-IR* lines were lethal, yielding no or few progeny (Figure 1E and Table S1D). Gene Ontology (GO) and GO gene set enrichment analysis of the total screen data (Figures S1C–S1D and Tables S1E and S1F) showed a significant enrichment of genes involved in ATP synthesis,

revealed significant enrichment for oxidative phosphorylation, amino acid and fatty acid metabolism, ubiquitin-mediated proteolysis, and various signaling pathways such as Wnt, ErbB, hedgehog, JAK-Stat, Notch, mTOR, or TGF $\beta$  (Table S1I). Thus, our thermal nociception screen and the subsequent bioinformatic analyses have revealed multiple genes and pathways that relate to the expression of an innate nociceptive behavior, many of which had no previous functional annotations.

### **straightjacket Is a Thermal Nociception Gene in *Drosophila***

One of the genes that we picked up in this screen was *straightjacket* (CG12295, *stj*), a member of the  $\alpha 2\delta$  family of genes that function as subunits of voltage-gated  $\text{Ca}^{2+}$  channels (Figure 2A) and control the function and development of synapses (Catterall, 2000; Dickman et al., 2008; Eroglu et al., 2009; Kurshan et al., 2009; Ly et al., 2008). The fly *stj* ortholog in mammals is  $\alpha 2\delta 3$ , a close homolog of  $\alpha 2\delta 1$ , which is the molecular target of gabapentin and pregabalin (Field et al., 2006), widely used analgesics for neuropathic pain in humans (Dworkin et al., 2007).

We confirmed that *stj* is required for noxious heat avoidance in adult *Drosophila* using a second independent hairpin (Figure 2B). The two *stj* hairpins resulted in about 90% and 60% reduction of *stj* mRNA expression, respectively (Figure 2C). Importantly, when flies were exposed to 46°C without a choice to escape, *stj* knockdown did not alter the kinetics of temperature-induced

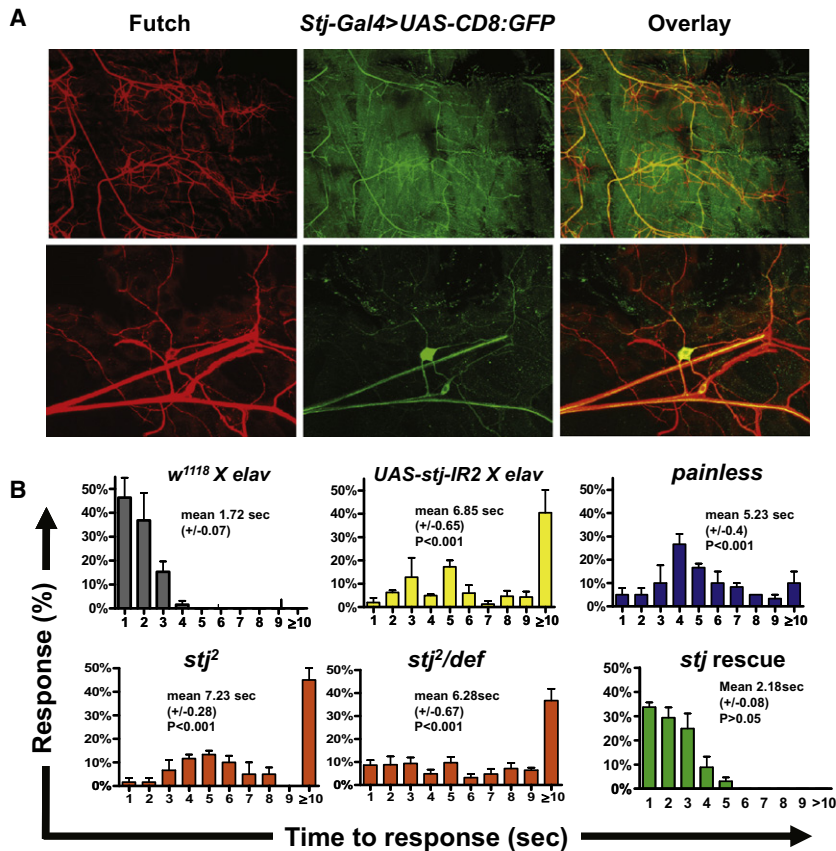


**Figure 3. Straightjacket Controls Thermal Nociception in *Drosophila* Larvae**

(A) *stj-GAL4*-driven expression of *UAS-CD8:GFP* in larval body wall sensory neurons costained with anti-Futsch as a marker for sensory neurons. CD8:GFP expression colocalizes with sensory neurons (Futsch) in larval abdominal hemi-segments (A3) (top) and multidendritic sensory neurons (bottom).

(B) Panneuronal knockdown of *stj* (*UAS-stj-IR* × *elav*), a mutant of *stj* (*stj<sup>2</sup>*), and *stj* mutant larvae over a corresponding deficiency *Df(2R)Exel7128* (*stj<sup>2</sup>/def*) show severely impaired thermal nociception responses compared to *w<sup>1118</sup>* × *elav* controls. *painless* larvae are shown as a control. The impaired larval thermal responses of a *stj/def* were rescued by reintroducing a wild-type *stj* allele using the P[acman] system (*stj<sup>2</sup>/def*, *stj<sup>+</sup>*) (Venken et al., 2009). Percent responses ± SEM to a 46°C heated probe are shown for the indicated time points. Mean response latency ± SEM. p value was generated using a Kruskal-Wallis nonparametric test for median comparison with the Dunn's post hoc test. All p values depicted highlight significance relative to control responses. *stj* rescue was also significantly different from *stj<sup>2</sup>* and *stj<sup>2</sup>/def* ( $p < 0.001$ ). At least 20 animals were tested three times per genotype.

See also Figure S3.

Larvae carrying a *stj* point mutation and the *stj* point mutation over a corresponding deficiency (*stj/def*) also exhibited impaired thermal nociception. The extent of the defective thermal pain response was greater at

paralysis (Figure 2D), indicating a specific deficit in the nociception response. Of note, *stj* knockdown had no overt effect on brain morphology (Figure S2A). Using a *stj-Gal4* line (Ly et al., 2008) driving *UAS-Lamin:GFP* to mark nuclei (Stuurman et al., 1999), we found GFP expression primarily in neurons in the pars intercerebralis and surrounding the subesophageal ganglion (Figure 2E and Figure S2B). *stjGAL4* > *UAS-CD8:GFP* labeling of axons (Lee and Luo, 1999) revealed broad projections throughout the central brain (Figure 2E and Figure S2B). Using antibodies raised against the *Drosophila* STJ protein, we confirmed STJ expression in *stjGAL4* > *UAS-Lamin:GFP*-positive cells of the pars intercerebralis (Figure 2F and data not shown). We also found GFP<sup>+</sup> nuclei and projections in the ventral nerve cord (VNC) and ascending/descending axons from the VNC that innervate the central brain (Figure S2C). *stj*-specific in situ hybridization revealed *stj* transcripts in the sensory organ (sensilla) of the leg (Figure 2G), indicating expression in the peripheral and central nervous system of the fly. Further studies are required to fine map the site of *stj* action in the *Drosophila* pain circuit.

We next assessed whether *stj* also controls thermal nociception in the larval heat pain paradigm (Tracey et al., 2003). In larvae, we found expression of *stj-Gal4* > *UAS-CD8:GFP* in multidendritic sensory neurons (Figure 3A). Panneuronal knockdown of *stj* (*UAS-stj-IR* × *elav-Gal4*) abrogated the larval response to noxious heat to an extent even greater than *painless* (Figure 3B).

higher temperatures (Figure S3A). Restoring a functional copy of *stj* using the P[acman] system (Venken et al., 2009) rescued the thermal nociception defects in *stj<sup>2</sup>* mutant larvae, confirming the requirement for *stj* in this behavior (Figure 3B and Figure S3A). *stj<sup>2</sup>* mutant larvae showed wild-type responses to nonnoxious touch (Kernan et al., 1994), indicating that these larvae are capable of responding to innocuous stimuli (Figure S3B). Collectively, these data show that *stj* is required for avoidance of noxious heat in *Drosophila*.

### Thermal Analgesia in $\alpha 2\delta 3$ Mutant Mice

We next tested whether the fly *stj* data is predictive of altered nociceptive behavior in mammals. The closest *stj* ortholog in mammals is  $\alpha 2\delta 3$  (mouse  $\alpha 2\delta 3$  is 33% identical and 60% similar to the STJ protein, and the domain structures are conserved throughout evolution [Ly et al., 2008]). To examine the role of  $\alpha 2\delta 3$  in vivo, we studied  $\alpha 2\delta 3$  mutant mice generated by homologous recombination. Correct recombination and loss of protein expression were confirmed by Southern (Figure 4A) and western blotting (Figure 4B).  $\alpha 2\delta 3$  mutant mice are born at the expected Mendelian frequency and are fertile. Extensive characterization of these mice showed no obvious anatomical or histological abnormalities, including apparently normal brain morphology (Tables S2A and S2B). There were also no genotype-related or biologically significant differences noted between age- and gender-matched mutant and wild-type control mice for any of

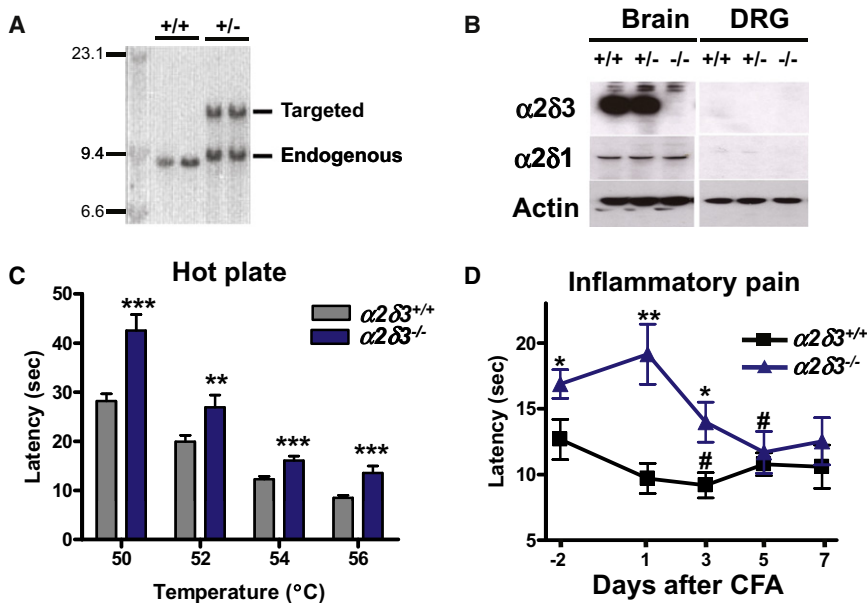


**Figure 4.  $\alpha 2\delta 3$  Is Required for Thermal Pain Responses in Mice**

(A) Southern blotting of genomic DNA in  $\alpha 2\delta 3$  wild-type (+/+) and  $\alpha 2\delta 3$  heterozygous (+/-) ES cells to confirm successful gene targeting. The endogenous wild-type and targeted alleles are indicated. A 5' probe was used on Nhe I digested genomic DNA.

(B)  $\alpha 2\delta 3$  and  $\alpha 2\delta 1$  protein expression in brain and isolated DRG lysates from  $\alpha 2\delta 3^{+/+}$  (+/+),  $\alpha 2\delta 3^{+/-}$  (+/-), and  $\alpha 2\delta 3^{-/-}$  (-/-) mice. Actin is shown as a loading control.

(C) Using the hot plate assay,  $\alpha 2\delta 3$  mutant mice (n = 16) show a delayed acute thermal nociception response as compared to control  $\alpha 2\delta 3^{+/+}$  mice (n = 12). Littermate mice were used as a control. Values represent the latency (seconds) to respond to the indicated temperatures.

(D) CFA-induced inflammatory pain behavior. CFA (20  $\mu$ l) was injected into the hindpaw of  $\alpha 2\delta 3^{+/-}$  (+/+, n = 10) and  $\alpha 2\delta 3^{-/-}$  (-/-, n = 21) littermates, and mice were tested for thermal pain (54°C) using the hot plate assay on the indicated days. Days 1, 3, 5, and 7 indicate days after CFA injection. All data are presented as mean values  $\pm$  SEM. \*p < 0.05; \*\*p < 0.01; and \*\*\*p < 0.001 comparing mutant versus control mice. #p < 0.05 comparing sensitization to baseline (day -2) of the same genotype (Student's t test). See also Figure S4 and Table S2.

the parameters evaluated at necropsy or by serum chemistry and hematology (Tables S2C and S2E). Moreover, normal growth and body weights were recorded for mice at 49, 90, 180, and 300 days of age (Table S2F). Hence, by all anatomical and physiological parameters assessed,  $\alpha 2\delta 3$  mutant mice appear normal.

Importantly, similar to *Drosophila stj* mutants,  $\alpha 2\delta 3$  mutant mice showed a defect in acute thermal nociception in the hot plate assay, with diminished responsiveness at 50, 52, 54, and 56°C (Figure 4C). In addition,  $\alpha 2\delta 3$  mutant mice exhibited delayed thermal sensitization in the Complete Freund's Adjuvant (CFA) model of peripheral inflammatory pain (Figure 4D), indicating that  $\alpha 2\delta 3$  contributes to the acute phase of heat hyperalgesia. CFA induced inflammation, as determined by paw swelling, was comparable between  $\alpha 2\delta 3$  mutant and control mice (Figure S4A). By contrast, mechanical sensitivities (von Frey test) were unaffected in  $\alpha 2\delta 3$  mutant mice (Figure S4B).  $\alpha 2\delta 3$  mutant mice were also evaluated for other behavioral tasks (Crawley, 2008): open field test to assess locomotor activity, general exploratory behavior, intrasession habituation, and general anxiety; tail suspension to assess behavioral despair; and a rotarod test to assess basic motor skills and coordination. In these assays, no significant differences were observed between  $\alpha 2\delta 3$  mutant and control mice (Figures S4C–S4F and Table S2G). Thus, genetic deletion of  $\alpha 2\delta 3$  in mice results in substantially impaired acute heat pain responses and a delay in inflammatory heat hyperalgesia.

#### $\alpha 2\delta 3$ SNPs Associate with Human Pain Sensitivity

Because knockdown of *straightjacket* in *Drosophila* and knockout of  $\alpha 2\delta 3$  in mice result in impaired sensitivity to thermal

pain, we speculated that polymorphisms at the  $\alpha 2\delta 3$  (*CACNA2D3*) locus might be associated with heat pain variance in humans. To assay for potential association of  $\alpha 2\delta 3$  haplotypes relative to pain sensitivity, we screened four single-nucleotide polymorphisms (SNPs) within or close to the human *CACNA2D3* gene (Figure 5A) in a cohort of 189 healthy volunteers subjected to a battery of experimental pain sensitivity tests (Diatchenko et al., 2005). Of these, the minor allele of the SNP rs6777055 was significantly associated with reduced thermal pain sensitivity, i.e., heat wind-up pain (Figure 5B, recessive model). Wind-up measures successive increases in perceived pain intensity to a repeated noxious heat stimulus (10 heat pulses of 1.5 s each at 50°C, each separated by 3 s).

Thermosensitive neurons have been also implicated in chronic pain in humans (Premkumar, 2010). To explore this, we compared pain levels in 169 Caucasian adults who participated in a prospective observational study of surgical discectomy for persistent lumbar root pain, caused by an intervertebral disc herniation (Atlas et al., 2001) for an association with *CACNA2D3* SNPs. The minor alleles of two *CACNA2D3* SNPs (rs1851048 and rs6777055) were associated with less pain within the first year following surgery (Figure 5C, recessive model). Importantly, the rs6777055 SNP C/C was significantly associated with less pain in both healthy volunteer and chronic pain cohorts showing a recessive mode of inheritance. In both the experimental and lumbar pain groups, the minor allele frequency for rs6777055 was 0.2; that is, ~4% of the human population is homozygous for this genetic variant. These data show that minor variants within the human *CACNA2D3* gene are associated with less heat-induced pain in healthy volunteers and reduced chronic pain in lumbar back pain patients.

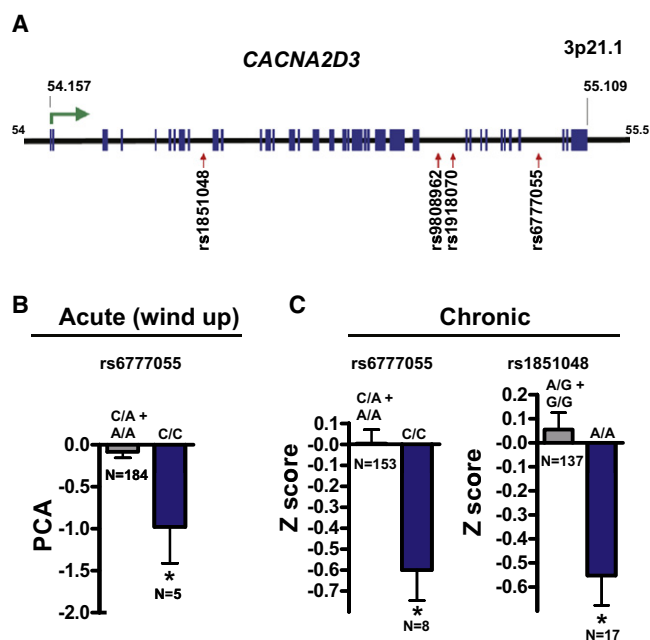


**Figure 5. Polymorphisms in *CACNA2D3* ( $\alpha 2\delta 3$ ) Associate with Decreased Acute and Chronic Pain in Humans**

(A) Schematic representation of the human *CACNA2D3* gene locus on chromosome 3p21.1. The positions of the SNPs assayed are indicated. Blue boxes represent exons. The relative gene position is given in megabases (Mb).

(B) Homozygous carriers of the rs6777055 minor allele (C/C) were significantly less sensitive to heat wind-up-induced sensitivity relative to the other genotypes (C/A or A/A).

(C) Of 169 lumbar chronic root pain patients, 1 year postdiscectomy, those homozygous for the minor allele C/C at SNP rs6777055 and A/A at SNP rs1851048 were less sensitive than the other allele combinations. In each case, the homozygous minor allele is associated with significantly less pain. Note that genotyping was not always successful for every individual, hence the slightly different total numbers in the chronic pain group. All data are presented as mean values  $\pm$  SEM. \* $p < 0.05$  (Student's *t* test).

### $\alpha 2\delta 3$ Controls Central Transmission of Pain Signals to the Sensory Cortex and Other Higher-Order Pain Centers

Nociceptive processing involves the relay of sensory information from primary nociceptor neurons to second-order neurons in the dorsal horn of the spinal cord that then transfer nociceptive information to the brain stem, thalamus, and higher-order brain centers (Costigan et al., 2009; Lumpkin and Caterina, 2007; Tracey and Mantyh, 2007). Because our  $\alpha 2\delta 3$  knockout mice carry a LacZ reporter, we used  $\beta$ -Gal staining as a marker to assess  $\alpha 2\delta 3$  expression. In the brain,  $\beta$ -Gal labeled the thalamus, pyramidal cells of the ventro-posterior paraflocculus of the cerebellum, caudate, putamen, the dentate gyrus of the hippocampus, and the olfactory bulb and tubercle, as well as diffusely throughout the cortex (Figure 6A and data not shown). The LacZ expression profiles were confirmed by western blotting and quantitative PCR (data not shown) and matched in situ data from the Allen brain atlas (data not shown and Koester and Insel, 2007). We failed to detect LacZ expression in the spinal cord and DRG (data not shown). Absence of  $\alpha 2\delta 3$  expression in primary

sensory DRG neurons was confirmed by western blotting (Figure 4B). In line with these expression data, our behavioral experiments showed that loss of  $\alpha 2\delta 3$  does not affect the noxious heat-induced tail flick response (Figure S4G), a pain behavior mediated by a spinal reflex circuit (Pitcher et al., 1995). Finally, patch clamping showed that calcium current and kinetics were comparable among DRG neurons from control and  $\alpha 2\delta 3$  mutant mice (Figures S4H–S4K), indicating no requirement for  $\alpha 2\delta 3$  in calcium channel function in these cells. These data suggest that  $\alpha 2\delta 3$  is not required for thermal pain processing in nociceptors and the spinal cord, but  $\alpha 2\delta 3$  may regulate thermal pain processing in the brain.

To address this, we employed noninvasive functional magnetic resonance imaging (fMRI) using the blood oxygenation level-dependent (BOLD) signal to generate activation maps of brain regions affected by noxious topical heat stimuli (Knabl et al., 2008; Ogawa et al., 1990; Thulborn et al., 1982). In wild-type mice ( $n = 20$ ), noxious thermal stimuli activate brain structures known as the “pain matrix” (Melzack, 1999) such as the thalamus (Figure 6B), the S1 and S2 somatosensory cortex (Figure 6C), the cingulum, amygdala, hypothalamus, or the motor cortex (Figure S5). These areas are also involved in pain perception in human subjects (Tracey and Mantyh, 2007). In both wild-type ( $n = 20$ ) and  $\alpha 2\delta 3$  mutant mice ( $n = 18$ ), thermal pain induced activation of the thalamus (Figure 6B), the key subcortical pain relay center (Price, 2000). Intriguingly, loss of  $\alpha 2\delta 3$  expression interrupted the normal engagement of pain circuitry in the brain, resulting in markedly reduced BOLD peak amplitudes and activation volumes in higher-order pain centers such as the somatosensory S1 and S2 cortices, cingulate, or motor cortex after exposure to noxious temperatures (Figure 6C and Figure S5). Impaired activation of higher-order pain centers, i.e., sensory and motor cortices, was confirmed by calculation of Euclidian distances (data not shown).

To additionally assess temporal information flow of the pain signal within different cerebral structures, we calculated a cross-correlation matrix of the response time profiles for each predefined region of the somatosensory pain matrix (Figure 6D). In control mice, the sensory input relays thermal-evoked neural signals to the thalamus, where it effectively spreads to other central brain centers such as the sensory and association cortex, limbic system, cerebellum, basal ganglia, and motor cortex.  $\alpha 2\delta 3$  mutant mice again exhibited normal activation of the thalamus but a reduced flow to nearly all of the higher-order pain centers, in particular the somatosensory cortex (SC) (Figure 6D). Moreover, whereas the pain signal spreads from the left (i.e., contralateral to the side of stimulation) in control mice, we found a considerable reduction in correlation coefficients of the pain signal from the left to the right brain in  $\alpha 2\delta 3$  mutant mice (Figure S6A). In addition, we observed increased negative BOLD signals in the S1 somatosensory, the motor, and the cingulate cortex on both hemispheres of  $\alpha 2\delta 3$  mutant mice (Figure S6B), suggesting that genetic inactivation of  $\alpha 2\delta 3$  not only results in impaired transmission of the signal to higher pain structures, but also in intracortical inhibition (Arthurs and Boniface, 2002; Shmuel et al., 2002). Thus, loss of  $\alpha 2\delta 3$  leads to impaired transmission of noxious heat-evoked signals from the thalamus to higher pain centers.

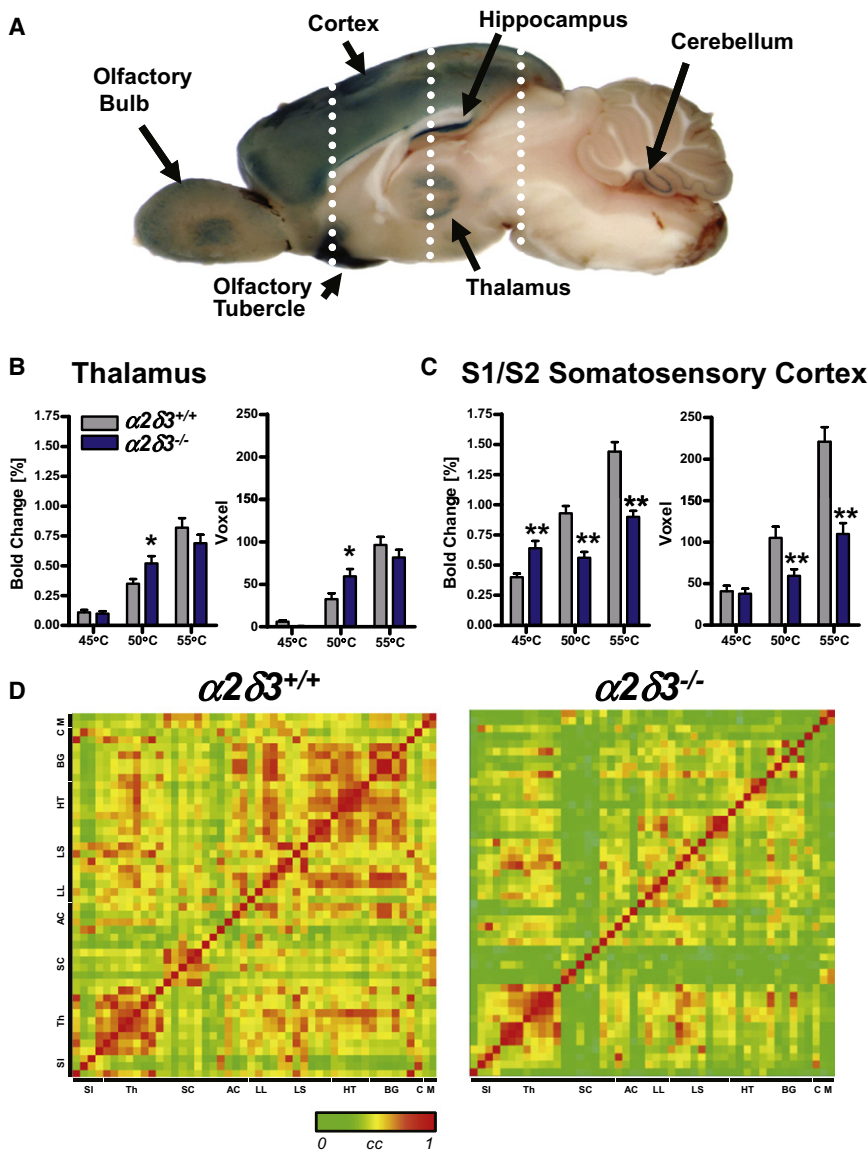


**Figure 6.  $\alpha 2\delta 3$  Is Expressed in the Brain and Relays the Pain Signal to Higher-Order Brain Centers**

(A)  $\beta$ -Gal staining of whole brain slices from  $\alpha 2\delta 3^{+/-}$  mice that carry the LacZ cassette. Different brain regions that are positive for LacZ expression are indicated. White lines indicate the brain slices displayed in Figure 7A.

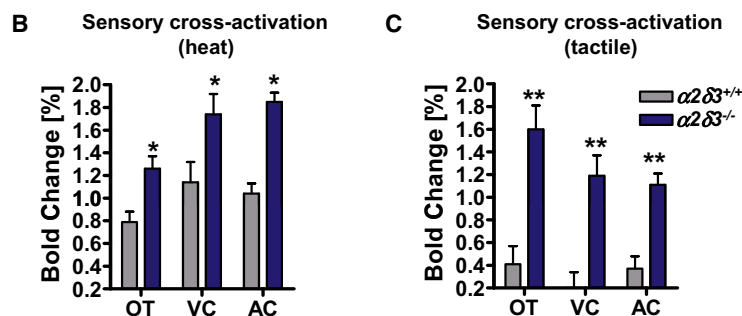
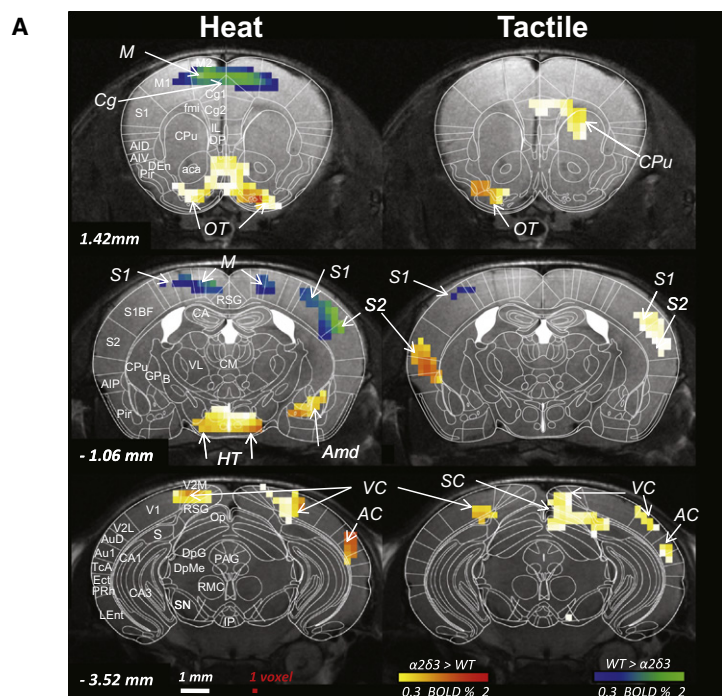
(B and C) Quantification of percent of BOLD change and mean activation volume (in voxels) for (B) the thalamus and (C) the S1 somatosensory cortex of  $\alpha 2\delta 3^{+/-}$  and  $\alpha 2\delta 3^{-/-}$  mice. Of note, it has been proposed that the S1 cortical region is involved in the localization of nociception (Treede et al., 1999). The different stimulation temperatures are indicated. Data are presented as mean  $\pm$  SEM. \* $p < 0.05$ ; \*\* $p < 0.01$  (Student's t test comparing the respective control and  $\alpha 2\delta 3^{-/-}$  groups).

(D) Cross-correlation matrix of time profiles. Whereas the pain signal spreads from the thalamus to other higher-order pain centers in  $\alpha 2\delta 3^{+/-}$  mice (red areas), in  $\alpha 2\delta 3^{-/-}$  mice, correlated activation can only be observed up to the level of the thalamus. Very weak activity is found in somatosensory cortex (SC) for  $\alpha 2\delta 3^{-/-}$  mice (green stripes). Data from the structures of the left side of the brain are shown following challenge with noxious heat (55°C) at the right hindpaw. SI, sensory input; Th, thalamus; SC, somatosensory cortex; AC, association cortex; LL, link to limbic system; LS, limbic system; HT, hypothalamus; BG, basal ganglia; C, cerebellum; M, motor cortex; P, periaqueductal gray. Correlation coefficients (cc) are given in the range from 0 (green) to +1 (red).  $n = 20$  for  $\alpha 2\delta 3^{+/-}$ ;  $n = 18$  for  $\alpha 2\delta 3^{-/-}$ . See also Figures S5 and Figure S6.

**Loss of  $\alpha 2\delta 3$  Results in Sensory Cross-Activation**

Although we found a marked impairment in the activation of known higher-order pain centers, one puzzling finding from our fMRI data was that we did not find statistically significant differences between control and  $\alpha 2\delta 3$  mutant mice in total activation volume and peak height when neuronal activity was surveyed in the entire brain (Figure S7A). Because we had initially only focused on the pain matrix, we speculated that, therefore, loss of  $\alpha 2\delta 3$  may result in hyperactivation of additional brain regions. Remarkably, noxious heat stimulation of all  $\alpha 2\delta 3$  mutant mice triggered significantly enhanced activation of the visual cortex and the auditory cortex, as well as olfactory brain regions (Figures 7A and 7B). Thus, in  $\alpha 2\delta 3$  mutant mice, noxious heat stimulation results in a significant sensory cross-activation of brain regions involved in vision, hearing, and olfaction.

stimulus-induced sensory cross-activations are not due to altered basal neuronal activity. Moreover, diffusion tensor imaging (DTI) showed no overt structural changes with respect to fractional anisotropy between the thalamus and higher-order pain centers or the thalamus and the visual, auditory, and olfactory centers. Further, cross-correlation analysis of the time profiles of the structures of the pain matrix from resting state BOLD imaging showed no defects in spontaneous spreading from the thalamus to higher-order pain centers in  $\alpha 2\delta 3$  mutant mice (data not shown). Finally, network analysis of this resting state brain activity showed no overt changes in total functional connectivity within the pain matrix (1087 connections in wild-type versus 1040 connections in  $\alpha 2\delta 3$  mutant mice) and also apparently normal multisensory-thalamo-cortical network connectivity (1922 connections in wild-type versus 2099 connections in  $\alpha 2\delta 3$  mutant mice). Although we cannot exclude subtle



developmental changes in defined neuronal populations of  $\alpha 2\delta 3$  mutant mice, these data suggest that the observed heat-induced sensory cross-activations (and defective transmission of the thermal pain signal from the thalamus to higher-order pain centers) are not due to altered basal neuronal connectivities.

To assess whether loss of  $\alpha 2\delta 3$  also results in sensory cross-activation in other sensory modalities, we performed BOLD imaging in response to tactile vibrissal stimulation (Hess et al., 2000). Among control and  $\alpha 2\delta 3$  mutant mice, we observed apparently normal activation of the brain region that encompasses the barrel field (data not shown); the barrel field is the primary cortical somatosensory brain center for processing of vibrissal stimulation (Petersen, 2007). Remarkably, although we observed apparently normal activation of the barrel field, tactile stimulation again resulted in sensory cross-activation of visual, auditory, and olfactory brain centers in  $\alpha 2\delta 3$  knockout mice (Figures 7A and 7C). Thus, in  $\alpha 2\delta 3$  mutant mice, noxious heat stimulation, as well as tactile stimulation, trigger sensory cross-activation of brain regions involved in vision, hearing, and olfaction.

### Figure 7. $\alpha 2\delta 3$ Mutant Mice Exhibit Sensory Cross-Activation in Response to Thermal and Tactile Stimuli

(A) Second-order statistical parameter maps showing only the significant differences of heat (55°C) and tactile (vibrissae) stimulation-induced brain activation between  $\alpha 2\delta 3^{+/+}$  and  $\alpha 2\delta 3^{-/-}$  mutant mice. Activation was assessed by BOLD-fMRI. The three planes correspond to the white lines shown in Figure 6A. The green/blue scale indicates increased peak activation (55°C) in  $\alpha 2\delta 3^{+/+}$  control mice compared to  $\alpha 2\delta 3^{-/-}$  mutant mice. The yellow/red scale indicates increased activation in  $\alpha 2\delta 3^{-/-}$  mutant mice compared to  $\alpha 2\delta 3^{+/+}$  control mice. Images depict significant differences of second-order group statistics corrected for multiple comparisons over all mice tested (n = 20 for  $\alpha 2\delta 3^{+/+}$  mice; n = 18 for  $\alpha 2\delta 3^{-/-}$  mice). Arrows point to activated regions; note that, for heat stimulation, the S1/S2 somatosensory cortex, the cingulate (Cg) cortex and the motor (M) cortex show significantly higher activity in  $\alpha 2\delta 3^{+/+}$  controls. In  $\alpha 2\delta 3^{-/-}$  mice, heat stimulation leads to significantly higher activity in the auditory cortex (AC), the visual cortex (VC), and the olfactory tubercle (OT), as well as the amygdala (Amd) and the hypothalamus (HT). For tactile stimulation, only one small region in the S1 somatosensory cortex, ipsilateral to the side of stimulation (right), showed significantly higher activity in  $\alpha 2\delta 3^{+/+}$  controls, whereas  $\alpha 2\delta 3^{-/-}$  mice again exhibited increased activation of the VC, AC, and OT, in addition to the caudate putamen (Cpu), S1, and S2 regions of the somatosensory cortex and the superior colliculus (SC).

(B and C) Percent of BOLD changes in the auditory cortex (AC), olfactory tubercle (OT), and visual cortex (VC) in control and  $\alpha 2\delta 3^{-/-}$  mice following (B) heat (55°C) and (C) tactile vibrissal stimulation. Data are presented as mean values  $\pm$  SEM. \*p < 0.05; \*\*p < 0.01 (Student's t test).

See also Figure S7.

## DISCUSSION

Our whole-genome, neuron-specific RNAi screen provides a global functional analysis of a complex, innate behavior. We have uncovered hundreds of candidate genes for thermal nociception, a large proportion of which had completely unknown functions until now. Because many of these genes are conserved across phyla, our data provide a starting point for large-scale human genomics efforts to finding novel pain genes and defining the molecular mechanisms of nociception.

One of the screen hits was the calcium channel subunit *straightjacket*/ $\alpha 2\delta 3$ . In both larva and adult *Drosophila*, we show that *straightjacket* is indeed required for heat nociception. Further work is required to define the spatial and temporal requirements for *stj* in thermal nociception. Importantly, similar to the fly, genetic deletion of  $\alpha 2\delta 3$  in mice also results in impaired acute heat pain responses. These results translate to humans because we found  $\alpha 2\delta 3$  polymorphisms that significantly associate with reduced heat pain sensitivity in healthy volunteers and lower levels of chronic pain in lumbar back pain patients. These data reinforce the extraordinary conservation of the neurobiological mechanisms of nociception, from its manifestation as avoidance of damage in primitive creatures like flies to the complex sensation of pain in humans.

Our functional imaging data indicate that  $\alpha 2\delta 3$  appears to be specifically required for central transmission of the thermal

nociceptive signal from the thalamus to the sensory cortex and other higher-order pain centers. Until now, it has been assumed that the threshold for thermal pain sensitization is set exclusively in peripheral sensory neurons via thermosensitive TRP channels like TRPV1 and altered excitability of nociceptor terminals (Hucho and Levine, 2007). However, our results indicate that noxious heat-evoked behavior is reduced even when nociception appears to be intact up to the thalamus. Whether the loss of  $\alpha 2\delta 3$  results in defective signaling and/or subtle alterations in synaptic circuits that link the thalamus to higher-order pain centers remains to be determined.

Intriguingly, in  $\alpha 2\delta 3$  mutant mice, thermal pain and tactile vibrissal stimulation triggered strong cross-activation of brain regions involved in vision, olfaction, and hearing. Sensory cross-activation, or synesthesia, is a neurological condition in which a stimulus in one sensory modality triggers perception of another sense (Hubbard and Ramachandran, 2005). In humans, synesthesia can be only objectively verified using functional brain imaging (Aleman et al., 2001). Multiple forms of synesthesia exist, including pain stimuli that trigger color (Dudycha and Martha, 1935). Synesthesia might affect up to 4% of the population, shows genetic linkage, and has been associated with intelligence and creativity (Hubbard and Ramachandran, 2005). In addition, thalamic lesions can also cause synesthesia (Beauchamp and Ro, 2008). Thus,  $\alpha 2\delta 3$  mutant mice might provide an animal model to enable the phenomenon of sensory cross-activation to be experimentally dissected.

## EXPERIMENTAL PROCEDURES

Detailed experimental procedures are provided in the [Supplemental Information](#).

### Fly Stocks

All *UAS-IR* transgenic fly lines were obtained from the VDRC RNAi library (Dietzl et al., 2007) with the exception of the second *stj* hairpin, which was obtained from the Harvard trip stocks. *elav* and *UAS-Dcr2* were gifts from B. Dickson (Dietzl et al., 2007). See [Extended Experimental Procedures](#) for a complete list of stocks used.

### Drosophila Behavioral Tests

For avoidance of noxious heat, ~20 4-day-old flies were placed in a sealed experimental chamber. All tests were performed in the dark. The bottom of the chamber was heated to 46°C, whereas the subnoxious zone was measured to be 31°C at the end of the 4 min experiment. Percent of avoidance was calculated by counting the number of flies that failed to avoid the noxious temperature compared to the total number of flies in the chamber. Larval pain assays were performed as described (Tracey et al., 2003). Mechanosensation (Kernan score) was performed as described (Kernan et al., 1994).

### Detection of *stj* Expression

Brains and ventral nerve cords of adult flies and sensory nerves of larvae from *stj-Gal4 > UAS-Lamin:GFP* (to detect nuclei) and *stj-Gal4 > UAS-CD8:GFP* (to detect axonal projections) lines were imaged. *stj*-expressing neurons were further detected using antibody staining and in situ hybridization.

### Generation of $\alpha 2\delta 3$ Knockout Mice

For gene targeting of  $\alpha 2\delta 3$  in mice, a targeting vector was inserted into exon 15 of the murine  $\alpha 2\delta 3$  gene. Germline-transmitted F1 mice were backcrossed onto a C57BL/6 background. All behavioral and fMRI mouse studies were conducted in accordance with guidelines of the European Union Council (86/609/EU) and following Austrian regulations for the use of laboratory animals.

### Mouse Behavioral Experiments

For the hot plate assay, wild-type and  $\alpha 2\delta 3$  mutant littermate mice were tested for hot plate latency at 50°C–56°C. The mechanical pain test was performed by applying von Frey hairs to the dorsal surface of each hind paw until a hind limb withdrawal response was observed; the hair with the minimum bending force required to produce a response was recorded. Inflammatory thermal hyperalgesia was produced in the mouse right hind paw by intraplantar injection of CFA. Before and after CFA injection, nociceptive responses to heat were measured using the hot plate test (54°C). Paw swelling was measured to evaluate the inflammatory response elicited by CFA.

### Western Blotting

The following primary antibodies were used: mouse anti-Actin, dilution 1/1000; goat anti- $\alpha 2\delta 1$ , dilution 1/500, and rabbit anti- $\alpha 2\delta 3$ , dilution 1/500. To generate the anti- $\alpha 2\delta 3$  antibody, rabbits were immunized with the peptide VSERTIKETTGNAC conjugated to KLH. Secondary antibodies were used at a dilution of 1 in 5000.

### LacZ Expression

Tissues from 7- to 12-week-old heterozygote mice were analyzed for LacZ expression using X-Gal staining followed by Nuclear Fast Red counterstaining. For whole-mount brain staining, the brain was cut longitudinally, fixed, and stained using X-Gal. Tissues were fixed with buffered formaldehyde.

### fMRI and BOLD Imaging

Male mice were anesthetized with isoflurane and placed inside of a MR machine (Bruker BioSpec 47/40, quadratur head coil) under extensive physiological monitoring. The contact heat stimuli (40°C, 45°C, 50°C, and 55°C, plateau for 5 s after 15 s of heat increase) were applied at the right hind paw (presented at 3 min 25 s intervals, three times each temperature) using a custom-made computer-controlled Peltier heating device. For tactile stimulation, the C1 vibrissa of the mice was moved with an air-driven device integrated into a cradle shifting the vibrissa by an inverted comb with an amplitude of 5 mm at 7 Hz. A series of 750 sets of functional images (matrix 64 × 64, field of view 15 × 15 mm, slice thickness 0.5 mm, axial, 22 slices) were collected using the Echo Planar Technique (EPI, single shot: TR = 4000 ms, TE<sub>eff</sub> = 24 and 38 ms).

### SNP Mapping in Humans

We genotyped four single-nucleotide polymorphisms (SNPs) spaced evenly through  $\alpha 2\delta 3$  using the 5' exonuclease method (Tegeeder et al., 2006). For acute pain studies, we genotyped 189 normal volunteers who had previously been phenotyped for ratings of experimental pain (Diatchenko et al., 2005). All subjects gave informed consent following protocols approved by the UNC Committee on Investigations Using Human Subjects. Volunteers were phenotyped with respect to temporal summation of heat pain (i.e., wind-up). For chronic pain studies, we collected DNA from 169 Caucasian adults who participated in a prospective observational study of surgical discectomy for persistent lumbar root pain (Atlas et al., 2001). The primary endpoint was persistent leg pain over the first postoperative year. Genotype-phenotype associations for each SNP were sought by regression analysis. The collection of DNA and genetic analyses were carried out with the approval of the National Institute of Dental and Craniofacial Research institutional review board, and informed consent was obtained from all subjects.

### Statistical Analyses

For analysis of adult heat dose avoidance responses between and within control and painless flies, a two-way ANOVA was performed, followed by Tukey's post hoc test. For analysis of adult *Drosophila* avoidance response and RNAi knockdown efficiency, a Student's t test (with correction for multiple comparisons) was performed. For analysis of larval pain behavior, we have performed the Kruskal-Wallis nonparametric test for median comparison followed by the Dunn's post hoc test. For mouse behavior, a Student's t test was used. For fMRI, the mean activity of each activated brain structure was averaged across all significant activated voxels and subjected to t tests comparing  $\alpha 2\delta 3$  mutant and control mice. At the second-level group analysis, a standard analysis of variance (ANOVA) was performed for Z score maps

between the different mice genotypes. Areas of significant group activation differences ( $p < 0.05$ ) were used as masks to only show the calculated peak activation maps in these regions. For human studies, genotype-phenotype associations for each SNP were sought by regression analysis. Unless otherwise indicated, data are represented as mean values  $\pm$  SEM.

## SUPPLEMENTAL INFORMATION

Supplemental Information includes Extended Experimental Procedures, seven figures, and two tables and can be found with this article online at doi:10.1016/j.cell.2010.09.047.

## ACKNOWLEDGMENTS

We thank all members of our laboratories and the VDRC for helpful discussions and excellent technical support. We thank Ricardo de Matos Simoes for support with statistical analysis. We thank B.J. Dickson for elav/UAS Dicer 2 stocks.  $\alpha 2\delta 3$  mutant mice were generated by Deltagen (San Mateo, CA). J.M.P. is supported by grants from IMBA, the Austrian Ministry of Sciences, the Austrian Academy of Sciences, GEN-AU (AustroMouse), ApoSys, and an EU ERC Advanced Grant. A.C.K. is supported by National Institute of Health NRSA 1 F32GM086207-01. C.J.W. is supported by NIH NS039518 and NS038253. G.G.N. was supported by a Mary Curie IIF Fellowship and EuroThymaide. A.H. is supported by DFG 661/TP4 and BMBF (01EM0514, 01GQ0731, 0314102) and K.B. by the Doerenkamp Foundation for Innovations in Animal and Consumer Protection. P.A.G. is supported by NIH NS044232.

Received: March 8, 2010

Revised: August 9, 2010

Accepted: September 24, 2010

Published: November 11, 2010

## REFERENCES

- Aleman, A., Rutten, G.J., Sitskoorn, M.M., Dautzenberg, G., and Ramsey, N.F. (2001). Activation of striate cortex in the absence of visual stimulation: an fMRI study of synesthesia. *Neuroreport* 12, 2827–2830.
- Arthurs, O.J., and Boniface, S. (2002). How well do we understand the neural origins of the fMRI BOLD signal? *Trends Neurosci.* 25, 27–31.
- Atlas, S.J., Keller, R.B., Chang, Y., Deyo, R.A., and Singer, D.E. (2001). Surgical and nonsurgical management of sciatica secondary to a lumbar disc herniation: five-year outcomes from the Maine Lumbar Spine Study. *Spine* 26, 1179–1187.
- Basbaum, A.I., Bautista, D.M., Scherrer, G., and Julius, D. (2009). Cellular and molecular mechanisms of pain. *Cell* 139, 267–284.
- Beauchamp, M.S., and Ro, T. (2008). Neural substrates of sound-touch synesthesia after a thalamic lesion. *J. Neurosci.* 28, 13696–13702.
- Catterall, W.A. (2000). Structure and regulation of voltage-gated  $Ca^{2+}$  channels. *Annu. Rev. Cell Dev. Biol.* 16, 521–555.
- Costigan, M., Scholz, J., and Woolf, C.J. (2009). Neuropathic pain: A maladaptive response of the nervous system to damage. *Annu. Rev. Neurosci.* 32, 1–32.
- Cox, J.J., Reimann, F., Nicholas, A.K., Thornton, G., Roberts, E., Springell, K., Karbani, G., Jafri, H., Mannan, J., Raashid, Y., et al. (2006). An SCN9A channelopathy causes congenital inability to experience pain. *Nature* 444, 894–898.
- Crawley, J.N. (2008). Behavioral phenotyping strategies for mutant mice. *Neuron* 57, 809–818.
- Diatchenko, L., Slade, G.D., Nackley, A.G., Bhalang, K., Sigurdsson, A., Belfer, I., Goldman, D., Xu, K., Shabalina, S.A., Shagin, D., et al. (2005). Genetic basis for individual variations in pain perception and the development of a chronic pain condition. *Hum. Mol. Genet.* 14, 135–143.
- Dickman, D.K., Kurshan, P.T., and Schwarz, T.L. (2008). Mutations in a Drosophila  $\alpha 2\delta$  voltage-gated calcium channel subunit reveal a crucial synaptic function. *J. Neurosci.* 28, 31–38.
- Dietzl, G., Chen, D., Schnorrer, F., Su, K.C., Barinova, Y., Fellner, M., Gasser, B., Kinsey, K., Oettel, S., Scheiblauer, S., et al. (2007). A genome-wide transgenic RNAi library for conditional gene inactivation in Drosophila. *Nature* 448, 151–156.
- Dudycha, G.J., and Dudycha, M.M. (1935). A Case of Synesthesia: Visual-Pain and Visual-Audition. *J. Abnorm. Soc. Psychol.* 30, 57–69.
- Dworkin, R.H., O'Connor, A.B., Backonja, M., Farrar, J.T., Finnerup, N.B., Jensen, T.S., Kalso, E.A., Loeser, J.D., Miaskowski, C., Nurmikko, T.J., et al. (2007). Pharmacologic management of neuropathic pain: evidence-based recommendations. *Pain* 132, 237–251.
- Eroglu, C., Allen, N.J., Susman, M.W., O'Rourke, N.A., Park, C.Y., Ozkan, E., Chakraborty, C., Mulinyawe, S.B., Annis, D.S., Huberman, A.D., et al. (2009). Gabapentin receptor  $\alpha 2\delta$ -1 is a neuronal thrombospondin receptor responsible for excitatory CNS synaptogenesis. *Cell* 139, 380–392.
- Field, M.J., Cox, P.J., Stott, E., Melrose, H., Offord, J., Su, T.Z., Bramwell, S., Corradini, L., England, S., Winks, J., et al. (2006). Identification of the  $\alpha 2$ - $\delta$ -1 subunit of voltage-dependent calcium channels as a molecular target for pain mediating the analgesic actions of pregabalin. *Proc. Natl. Acad. Sci. USA* 103, 17537–17542.
- Hess, A., Stiller, D., Kaulisch, T., Heil, P., and Scheich, H. (2000). New insights into the hemodynamic blood oxygenation level-dependent response through combination of functional magnetic resonance imaging and optical recording in gerbil barrel cortex. *J. Neurosci.* 20, 3328–3338.
- Hubbard, E.M., and Ramachandran, V.S. (2005). Neurocognitive mechanisms of synesthesia. *Neuron* 48, 509–520.
- Hucho, T., and Levine, J.D. (2007). Signaling pathways in sensitization: toward a nociceptor cell biology. *Neuron* 55, 365–376.
- Kernan, M., Cowan, D., and Zuker, C. (1994). Genetic dissection of mechanosensory transduction: mechanoreception-defective mutations of Drosophila. *Neuron* 12, 1195–1206.
- Knabl, J., Witschi, R., Hösl, K., Reinold, H., Zeilhofer, U.B., Ahmadi, S., Brockhaus, J., Sergejeva, M., Hess, A., Brune, K., et al. (2008). Reversal of pathological pain through specific spinal GABAA receptor subtypes. *Nature* 451, 330–334.
- Koester, S.E., and Insel, T.R. (2007). Mouse maps of gene expression in the brain. *Genome Biol.* 8, 212.
- Kurshan, P.T., Oztan, A., and Schwarz, T.L. (2009). Presynaptic  $\alpha 2\delta$ -3 is required for synaptic morphogenesis independent of its  $Ca^{2+}$ -channel functions. *Nat. Neurosci.* 12, 1415–1423.
- Lee, T., and Luo, L. (1999). Mosaic analysis with a repressible cell marker for studies of gene function in neuronal morphogenesis. *Neuron* 22, 451–461.
- Lumpkin, E.A., and Caterina, M.J. (2007). Mechanisms of sensory transduction in the skin. *Nature* 445, 858–865.
- Ly, C.V., Yao, C.K., Verstreken, P., Ohyama, T., and Bellen, H.J. (2008). straightjacket is required for the synaptic stabilization of cacophony, a voltage-gated calcium channel  $\alpha 1$  subunit. *J. Cell Biol.* 181, 157–170.
- Manev, H., and Dimitrijevic, N. (2004). Drosophila model for in vivo pharmacological analgesia research. *Eur. J. Pharmacol.* 491, 207–208.
- Melzack, R. (1999). From the gate to the neuromatrix. *Pain Suppl.* 6, S121–S126.
- Ogawa, S., Lee, T.M., Kay, A.R., and Tank, D.W. (1990). Brain magnetic resonance imaging with contrast dependent on blood oxygenation. *Proc. Natl. Acad. Sci. USA* 87, 9868–9872.
- Petersen, C.C. (2007). The functional organization of the barrel cortex. *Neuron* 56, 339–355.
- Pitcher, G.M., Yashpal, K., Coderre, T.J., and Henry, J.L. (1995). Mechanisms underlying antinociception provoked by heterosegmental noxious stimulation in the rat tail-flick test. *Neuroscience* 65, 273–281.

- Premkumar, L.S. (2010). Targeting TRPV1 as an alternative approach to narcotic analgesics to treat chronic pain conditions. *AAPS J.* 12, 361–370.
- Price, D.D. (2000). Psychological and neural mechanisms of the affective dimension of pain. *Science* 288, 1769–1772.
- Shmuel, A., Yacoub, E., Pfeuffer, J., Van de Moortele, P.F., Adriany, G., Hu, X., and Ugurbil, K. (2002). Sustained negative BOLD, blood flow and oxygen consumption response and its coupling to the positive response in the human brain. *Neuron* 36, 1195–1210.
- Silva, A.C., Lee, J.H., Aoki, I., and Koretsky, A.P. (2004). Manganese-enhanced magnetic resonance imaging (MEMRI): methodological and practical considerations. *NMR Biomed.* 17, 532–543.
- Sokabe, T., Tsujiuchi, S., Kadowaki, T., and Tominaga, M. (2008). Drosophila painless is a Ca<sup>2+</sup>-requiring channel activated by noxious heat. *J. Neurosci.* 28, 9929–9938.
- Stuurman, N., Delbecq, J.P., Callaerts, P., and Aebi, U. (1999). Ectopic overexpression of Drosophila lamin C is stage-specific lethal. *Exp. Cell Res.* 248, 350–357.
- Tegeder, I., Costigan, M., Griffin, R.S., Abele, A., Belfer, I., Schmidt, H., Ehnert, C., Nejm, J., Marian, C., Scholz, J., et al. (2006). GTP cyclohydrolase and tetrahydrobiopterin regulate pain sensitivity and persistence. *Nat. Med.* 12, 1269–1277.
- Thulborn, K.R., Waterton, J.C., Matthews, P.M., and Radda, G.K. (1982). Oxygenation dependence of the transverse relaxation time of water protons in whole blood at high field. *Biochim. Biophys. Acta* 714, 265–270.
- Tracey, I., and Mantyh, P.W. (2007). The cerebral signature for pain perception and its modulation. *Neuron* 55, 377–391.
- Tracey, W.D., Jr., Wilson, R.I., Laurent, G., and Benzer, S. (2003). painless, a Drosophila gene essential for nociception. *Cell* 113, 261–273.
- Treede, R.D., Kenshalo, D.R., Gracely, R.H., and Jones, A.K. (1999). The cortical representation of pain. *Pain* 79, 105–111.
- Venken, K.J., Carlson, J.W., Schulze, K.L., Pan, H., He, Y., Spokony, R., Wan, K.H., Koriabine, M., de Jong, P.J., White, K.P., et al. (2009). Versatile P[acman] BAC libraries for transgenesis studies in Drosophila melanogaster. *Nat. Methods* 6, 431–434.
- Xu, S.Y., Cang, C.L., Liu, X.F., Peng, Y.Q., Ye, Y.Z., Zhao, Z.Q., and Guo, A.K. (2006). Thermal nociception in adult Drosophila: behavioral characterization and the role of the painless gene. *Genes Brain Behav.* 5, 602–613.